History of Medicine, 2023, 9(1): 1959–1969
DOI: 10.17720/2409-5834.v9.1.2023.252

Evaluation of the Biological Activity of Nickel oxide-Nanoparticles as antibacterial Staphylococcus aureus

Sarab Morad[1*], Laith A. Yaaqoob[2]

[1]Department of Biotechnology, College of Science, University of Baghdad, Iraq
Email: Sarab.morad1106a@sc.uobaghdad.edu.iq
[2]Department of Biotechnology, College of Science, University of Baghdad, Iraq
Email: Laith.yaaqoob@sc.uobaghdad.edu.iq

***Correspondence author:** Sarab Morad (Sarab.morad1106a@sc.uobaghdad.edu.iq)

Received: 23 January 2023 **Accepted:** 14 April 2023

Citation: Morad S, Yaaqoob LA (2023) Evaluation of the Biological Activity of Nickel Oxide-Nanoparticles as antibacterial Staphylococcus aureus. History of Medicine 9(1): 1959−1969. https://doi.org/10.17720/2409-5834.v9.1.2023.252

Abstract

Pathogenic strains frequently spread infections by producing virulence factors like potent protein toxins and the expression of a cell-surface protein that binds and inactivates antibodies. Staphylococcus aureus is one of the leading pathogens for deaths linked to antimicrobial resistance and the emergence of antibiotic-resistant strains. There is currently no licenced S. aureus vaccine, despite extensive research and development. Therefore, the aim of this study includes biosynthesize of Nickel oxide-nanoparticles (NiO-NPs) using Lepidium sativum aqueous plant leaves extract, and use of the biosynthesized nanoparticles as antibacterial and anti-biofilm against multi-drug resistant S. aureus. 150 samples of both sexes, ranging in age from 1 to 60 years, were randomly selected from 65 male and 85 female patients who had infected burns and wounds at various hospitals. After the final diagnosis of the clinical samples, 20 isolates of Staphylococcus aureus were obtained, then full identification of S. aureus using conventional biochemical tests. The antibiotic susceptibility test for fourteen antibiotics was performed by the standard well diffusion method, The results of the current investigation revealed that all S. aureus isolates varied in their resistance to the 14 antibiotics utilized in this study. Therefore, ten multi-drug resistant isolates of S. aureus were selected and examined their ability to form biofilm using the micro-titter plate method; the results revealed that eight isolates were strong in biofilm formation and two isolates were moderate. Maceration method was used to prepare Lepidium sativum aqueous plant leaves extract. Furthermore, NiO/NPs were prepared from the Lepidium sativum aqueous plant leaves extract and diagnose using ultraviolet (UV) spectroscopy, Field emission Scanning electron microscopy (FE-SEM), atomic fluorescence microscopy (AFM), X-ray scattering (XRD) and Fourier transformation infrared spectroscopy (FTIR). In addition, several experiments were conducted on the nanoparticles, including evaluation of antibacterial activity, biofilm formation and determination of the minimum inhibitory concentration. The diagnostic results showed that the nanoparticles are spherical in shape, single or combined, and crystalline for NiO-NPs and an average size of 42.27 nm. As the results showed that the NiO-NPs in concentration of 64 mg/ml was more effective than the NiO-NPs in concentration of 32 mg/ml, which gave the highest inhibition zone value of 15.67 mm. Furthermore, The result of the minimum inhibitory concentration (MIC) values of NiO-NPs on on all S. aureus isolates were 2 mg\ml except isolate 9 which was 4 mg\ml. As for the anti-biofilm activity on S. aureus isolates the results showed of NiO-NPs inhibit 100% in concentration 2 mg/ml of the biofilm formation From the results obtained in this study, several conclusions were concluded as the following, Staphylococcus aureus isolates showed high resistance to All antibiotics used in the study. It can also synthesiz of NiO-NPs by extracted from Lepidium sativum aqueous plant leaves extract, and the synthesized NiO-NPs have significant antibacterial S. aureus agent, it also inhibits of the formation biofilms in S. aureus depending on the concentration used. More studies should be conducted about the antibacterial activities of NiO-NPs on the other microorganisms associated with different human infections, and conduct more studies of NiO-NPs on immunological and cancer cell lines due to their effectiveness as an antioxidant.

Keywords

NiO-nanoparticles, antibacterial activity, Lepidium sativum, FTIR, AFM, FE-SEM, UV and XRD.

The study of science, engineering, and technology at the nanoscale, or between 1 and 100 nm, is known as nanotechnology. This cutting-edge technology is employed in a variety of areas, including chemistry, materials science, and others of a same kind. Additionally, numerous varieties of nanoparticles are applied in medicine as imaging agents or medication carriers. Different produced liposome nanoparticle kinds are now employed as vaccination and anti-cancer medication delivery systems. Additionally, gold nanoparticles are utilized in home pregnancy test kits [1-2].

Chemical procedures are recognized to be riskier than green synthesize. This is so that the latter can produce nanoparticles in a manner that is acknowledged as being more environmentally benign and sustainable (NPs) [3]. Some of the unique green methodologies, such as the emerging green nanotechnology, have shown to be crucial in the production of newer nanoparticles. These alternate approaches, which have shown to be more successful in producing NPs are those that incorporate microbes and plant extracts [4].

Explaining the dimensional progression of many physical traits and some previously undetected elements is a growing topic of innovative knowledge production. Basic and applied scientific fields have been quickly developed inside the empirical discipline of various nanotechnologies [5]. Nanotechnology is anticipated to accelerate technological advancements across a range of fields and has great promise for making a number of ground-breaking discoveries in the near future [6].

Although there are many metals in nature, but they are manufactured on a large scale by using a few of them such as gold, silver, palladium, nickel and platinum in the form of nanostructures [7].

The biological activity of several metal oxides has recently been studied, particularly in the biomedical disciplines. Among these, nickel oxide (NiO) was found to be reasonably priced, photo-stable, widely accessible, and not harmful to people when used in short-term exposure [8]. By analyzing the manufactured NiO-NPs in vitro, researchers found that they can primarily be employed as antibacterial medicines against a wide variety of Gram-positive and Gram-negative bacteria [9].

Materials and methods

Synthesize of nickel oxide-nanoparticles by Lepidium sativum aqueous plant leaf extract

Preparation of Lepidium sativum aqueous plant leaves extract

The Lepidium sativum leaves were removed, carefully cleaned, and chopped into small pieces. Then, 100 g of leaves were soaked with 500 ml of distilled water at 60 °C for 4 to 5 hours. The extract was then filtrated using a centrifuge for ten minutes at 10,000 rpm; the filtrate was used to prepare NPs [8].

Synthesize of nickel oxide-nanoparticles

All substances and reagents employed in the manufacture of NiO-NPs were bought from Sigma, Ltd, UAS, and the process given by Ezhilarasia et al. [9],], 1000 gram of young plant(Lepidium sativum) clean and mixed with distilled water in(60 °C)for 5 hours .Then mixing very well with blender (fruits mixer) and leave it 24 hours in room temperature. the extract was then filtrated using a centrifuge for ten minutes at 10,000 rpm.the liquid filtrate will be ready for prepare manganese oxide-nanoparticles . 25gram of nickel (II) sulphate ($NiSO_4.6H_2O$) was dissolved in 250 ml deionized distilled water and dispersed by an ultra-sonication bath for 10 minutes. The extract placed in a beaker glass for 24 hours inside the shaker ; the extract was then filtrated using a centrifuge for ten minutes at 10,000 rpm. The precipitate was collected and placed in glass dishes in an incubator for 48 to 72 hours in order to dry and grind it, thus the nanoparticles was ready to use. Then, various concentrations of the synthesized NiO-NPs were prepared.

Nanoparticles Characterization Techniques

UV-Visible Absorption Spectroscopy (UV-VIS) double-beam spectrophotometers were used to measure the absorbance spectra of the NiO-NPs solution. Atomic force microscopy (AFM) measurements of the average diameter crystalline size were used to show the generated NiO-NPs 2D and 3D topologies. Field emission scanning electron microscopy (FE-SEM) was used for further characterization. The X-ray diffraction patterns were used to determine the crystal structure (XRD). Fourier transformation infrared spectroscopy (FTIR) (Shimadzu) analysis was utilized to investigate the characterization of functional groups on the surface of NiO-NPs by plant extracts. As per standard procedures, the samples were created by spreading them out on a glass slide. Following that, the sample was examined; the preparation of NiO-NPs was performed in the Biotechnology Department, Nanotechnology Laboratory / College of Science / University of Baghdad / Iraq, while the characterization was conducted in the Chemistry Department / College of Science / University of Baghdad / Iraq.

Evaluation of antibacterial activity

Preparation of bacterial isolates

In this study, the isolated bacteria Staphylococcus aureus were collected From March 2021 to the end of November 2022, 150 samples of both sexes, ranging in age from 1 to 60 years were randomly selected from 65 male and 85 female patients who had infected burns and wounds at various hospitals. Before to the trials, all of the study's confirmation tests were carried out in the lab, where the diagnosis was verified using the VITEK-2 System. The bacteria were then activated by growing in nutrient broth and cultured for 24 hours at 37 °C to be utilized in studies to determine antibiotic activity.

Antibiotic susceptibility test

The Kirby-Bauer technique, as specified by the World Health Organization [10], was used to evaluate antibiotic susceptibility for 14 different antibiotics. Picking 1-2 isolated colonies of bacteria from the original culture and introducing them into a test tube containing 4 ml of normal saline produced a bacterial suspension with moderate turbidity compared to the 0.5 McFarland turbidity standard provides an optical density comparable to the density of a bacterial suspension 1.5x 10^8 colony forming units (CFU/ml). A portion of the bacterial suspension was transferred and gently and uniformly spread over Mueller-Hinton agar medium, then left for 10 minutes. Following that, the antimicrobial discs were firmly put on the agar to ensure contact with the agar. The plates were then inverted and incubated for 24 hours at 37°C. According to the Clinical Laboratories Standards Institute, inhibition zones formed around the discs were measured in millimetres (mm) using a metric ruler [11].

Assessment of biofilm formation

According to instructions to Patel et al. [12], S. aureus ability to quantitatively produce biofilms was evaluated. All isolates were cultured over-night in Brain Heart Infusion Broth at 37°C. Each isolate was added to tryptic soy broth (TSB), which contains 1% glucose, and well mixed. The turbidity of a suspension of the bacterial isolate was set to McFarland No. 0.5.

To a sterile, 96-well microtiter plate with a flat bottom, a volume (200 µl) of each isolate's culture was added in triplicate. With their covers on, the plate was incubated for 24 hours at 37°C under aerobic conditions. To get rid of the unattached bacteria after the incubation time, the planktonic cells were twice washed with distilled water. 200 µl of 100% methanol was used to fix the adhering bacterial cells in each well for 20 min at room temperature. 200 µl of 0.1% crystal violet was poured into each well and left there for 15 minutes to stain the adherent cells. After the staining process was finished, the additional stain was removed by repeated washing with distilled water (2−3 times). To ensure that the plate was dry, it was dried at room temperature for around 30 minutes. Next, 33% acetic acid was applied to remove the stain.

An ELISA auto reader operating at a wavelength of 630 nm was used to measure optical density (OD) values. All test results were computed, and the average of the OD values of the sterile medium was removed. Cut off value (ODc) was computed, and it may classify isolates as producing biofilms or not [13].

ODc: Average OD of negative control + (3 Ч standard deviation (SD) of Negative control),

OD isolate: Average OD of isolate − ODc. By the calculation of cutoff value (ODc), the result of biofilm is detected as below:

OD ≤ ODc (no biofilm production).

ODc < OD ≤ 2 Ч ODc (weak biofilm production).

2 Ч ODc < OD ≤ 4 Ч ODc (moderate biofilm production).

4Ч ODc < OD (strong biofilm production).

Study the antibacterial activity of nickel oxide-nanoparticles

Agar well diffusion method

The agar well diffusion method was employed for the determination of this study. Mueller- Hinton agar plates were swabbed (sterile cotton swabs) with broth culture (0.5 McFarland standard) of bacteria. Wells (6 mm diameter) were made in each of these plates using a sterile cork borer. 100 µl from each concentration (32 and 64 mg/ml) of the NiO-NPs were put in each hole by using a micropipette and allowed to diffuse at room temperature for 30 min. The plates were incubated at 37°C for 24 hours. The diameter of any resulting zone of inhibition was measured in millimeters [14].

Determination of Minimum Inhibitory Concentration (MIC) of nickel oxide-nanoparticles

The 96-well microtiter plate was used to determine the (MIC) of the NiO-NPs using the broth microdilution technique. The NiO-NPs working solution was prepared in broth at 64 mg/ml, and serial two-fold dilutions of NiO-NPs were prepared directly on the plate to make concentrations of (0.25, 0.5, 1, 2, 4, 8, 16, 32) mg/ml. 200 µl of the prepared NiO-NPs

put into the first row A wells. In columns, rows B to H contained 100 µl of the broth alone. Using a micropipette, twofold serial dilutions were performed methodically down the columns (from rows A to H). 100 µl was withdrawn from the starting concentrations in row A and transferred to the next row with the 100 µl broth, which was appropriately mixed, and the operation was repeated until the last row (H), when the last 100 µl was discarded. This brings the final volume in all the test wells with the NiO-NPs to 100 µl except the column which had 200 µl of the broth that served as sterility control. 100 µl of the $1.5Ч10^8$ CFU/ ml bacterial inoculum was transferred into all the wells except the negative control.

Microtiter plates were incubated for 24 hours at 37°C. Following incubation, 20 µl of resazurin dye was added to each well and leave for 30 minutes to see whether any color changes occurred. The Minimum Inhibitory Concentrations of the NiO-NPs at which no color changed from blue to pink in the resazurin broth test were measured visually in broth micro dilutions [15].

Study the anti-biofilm activity of nickel oxide-nanoparticles

The anti-biofilm activity of NiO-NPs was tested using a 96-well microtiter plate. The NiO-NPs working solution was created at 32 mg/ml for the NiO-NPs to make the concentrations (32, 16, 8, 4, 2, 1, 0.5 and 0.25) mg/ml. Only the first wells in row A contained 200 µl of each sample, whereas rows B through H had 100 µl of the broth. Twofold serial dilutions were carried out methodically down the columns (from rows A to H). 100 µl was drawn from the starting concentrations in row A and transferred to the next row with the 100 µl broth, which was properly mixed, and the operation was repeated until the last row (H), at which time the last 100 µl was discarded. Each well received 100 µl of the $1.5Ч10^8$ CFU/ ml bacterial inoculum, with the exception of the negative control. The same procedure as indicated in the paragraph was used (Assessment of biofilm formation).

Statistical analysis

This study employed one-way analysis of variance (ANOVA). Using SPSS version 23, the correlations and significance of the differences were assessed, and p values ≤ 0.01 were used to indicate statistically significant differences. Standard deviation was used to represent the data as mean ±.

Results and Discussion

Antibiotic susceptibility test

The results of the current investigation revealed that all S. aureus isolates varied in their resistance to the 14 antibiotics utilized in this study, which have been selected in accordance with (CLSI, 2019), which were tested for antibiotic sensitivity (Table 1). All (20) bacterial isolates showed resistance to the antibiotics Vancomycin, Azithromycin, and Ceftazidime, with a percentage of 100%. However, the percentage of bacterial resistance to antibiotics Imipenem and Cefotaxime were (90%). Additionally, with percentages of 65%, 55%, and 50%, respectively, the bacterial isolates demonstrated a rather high resistance to the antibiotics Amikacin, Trimethoprim, and Norfloxacin. The bacterial isolates under study recorded a relative sensitivity to some antibiotics, which are Gentamicin and Tobramycin, with a percentage of 65%, respectively, followed by Tetracycline, Ciprofloxacin, Trimethoprim/sulfamethoxazole and Levofloxacin with a percentage of 60%, 55%, 55% and 50%, respectively. Therefore, ten isolates of S. aureus that are highly resistant to antibiotics were selected for this study.

Table (1): Number of isolates and percentage of Staphylococcus aureus resistance to a number of antibiotics

Antibiotics	Symbol	Resistance (R)		Intermediate (I)		Sensitive (S)		Total (%)
		No.	(%)	No.	(%)	No.	(%)	
Cefotaxime (30 µg)	CTX	18	90	0	0	2	10	20 (100)
Imipenem (10 µg)	IPM	18	90	0	0	2	10	20 (100)
Ciprofloxacin (10 µg)	CIP	8	40	1	5	11	55	20 (100)
Levofloxacin (5 µg)	LEV	9	45	1	5	10	50	20 (100)
Trimethoprim (10 µg)	TM	11	55	1	5	8	40	20 (100)
Amikacin (10 µg)	AK	13	65	1	5	6	30	20 (100)
Vancomycin (10 µg)	VA	20	100	0	0	0	0	20 (100)
Azithromycin (15 µg)	AZM	20	100	0	0	0	0	20 (100)
Tetracycline (10 µg)	TE	8	40	0	0	12	60	20 (100)
Gentamycin (10 µg)	CN	6	30	1	5	13	65	20 (100)
Ceftazidime (30 µg)	CAZ	20	100	0	0	0	0	20 (100)
Norfloxacin (10 µg)	NX	10	50	0	0	10	50	20 (100)
Trimethoprim/ sulfamethoxazole (25 µg)	SXT	8	40	1	5	11	55	20 (100)
Tobramycin (10 µg)	TOB	6	30	1	5	13	65	20 (100)

The current study was considered to be somewhat consistent with some of the results of local and international studies. The researchers, Basil AbdulRazzaq et al. [16] found that Staphylococcus aureus isolated from different clinical models from Baghdad hospitals, that this bacterium was resistant to Azithromycin with a percentage of 61.4%, Gentamicin 24%, Levofloxacin 30%, Tetracycline 52.8%, and Vancomycin 14.2%.

Detection of biofilm formation

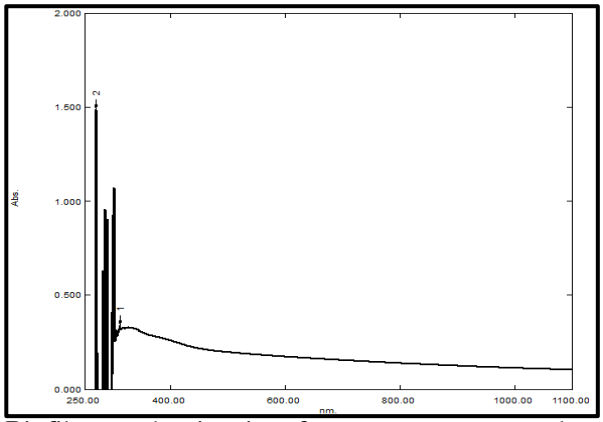

Biofilm production is a frequent strategy employed by bacteria to survive under harsh environmental conditions. Bacteria may form biofilms in water systems and on groups of abiotic surfaces often utilized in such systems, as well as in natural aquatic habitats [17]. The Microtiter plate was used to detect the quantitative of biofilm formation in order to quantify biofilm strength. The findings showed that all isolates had high biofilm formation except for isolates 9 and 10, which had moderate biofilm formation, The 10 best selected isolates as shown in (Table 2).

Table (2): Biofilm forming of S. aureus isolates

S. aureus isolates	S1	S2	S3	S4	S5	S6	S7	S8	S9	S10
Biofilm forming	Strong	Strong	Strong	Strong	Strong	Strong	Strong	Strong	Moderate	Moderate

(S): *S. aureus* isolates, Control negative (Cut off) = 0.2

Characterization of nickel oxide-nanoparticles

The following approaches have been used to evaluate the morphological, structural, and optical characteristics of synthesized NiO-NPs:

UV-Visible spectroscopy

Lepidium sativum aqueous plant leaves extract was combined with $NiSO_4.6H_2O$, which caused a change in colour. The stimulation of the metal nanoparticles' generated Surface Plasmon Resonance (SPR) vibrations led to the colour shift that was seen. The free electron that results from the conduction and valence bands of metal nanoparticles being near to one another is what causes the SPR. In the synthesis of NiO-NPs, a typical peak value is produced by the collective oscillation of free electrons of metal nanoparticles in resonance with the light wave. The colour shift made it simple to monitor the process and UV-Vis spectroscopy verified it.

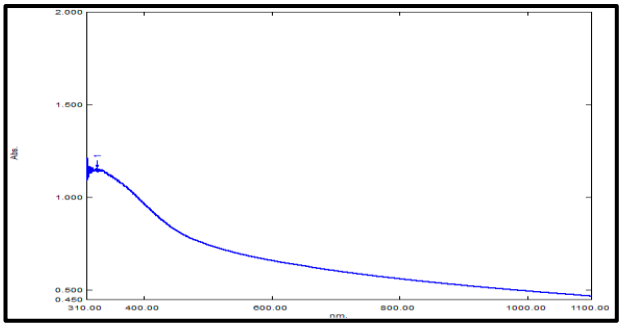

Figure (1): UV-Visible spectral analysis of Lepidium sativum aqueous plant leaves extract

Figures 1 and 2 show the UV-Vis spectra of aqueous plant extracts containing NiO-NPs. The modest absorption peak at 300 nm demonstrates the interaction of numerous chemical molecules with mineral ions [18].

The type, size, and morphologies of the NPs generated, the dielectric constant of the medium and temperature, as well as their inter-particle distances, all have a remarkable impact on the surface Plasmon resonance absorbance [19].

Nanoparticles have UV-visible absorption properties [20]. With a rise in NP concentration, the UV-visible absorption intensity of NPs typically rises [21]. In the present study the absorption spectrum was recorded between 250 nm and 1100 nm. In addition, it is observed that the nickel oxide-nanoparticles (NiO-NPs) surface Plasmon resonance band centered at 319 nm in comparison with UV Test for Lepidium sativum aqueous plant leaves extract 270 nm.

Field emission scanning electron microscopy (FE-SEM)

The shape and morphology of the generated green nanoparticles were examined using (FE-SEM), one of the extensively utilized methods for characterizing synthetic nanoparticles. The observations show that nanoparticle morphology is very varied, with a wide range of sizes and shapes.

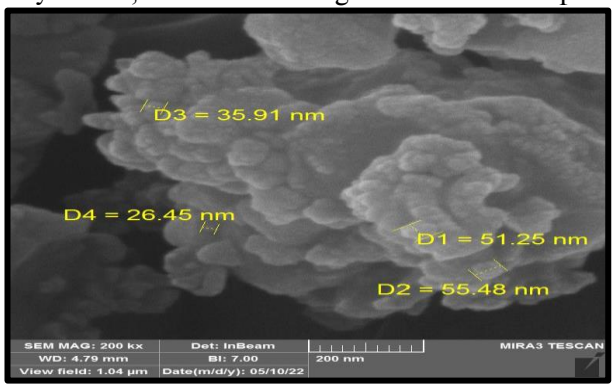

Figure (2): UV-Visible spectral analysis of NiO-NPs

A Field emission scanning electron microscopy (FE-SEM) has been used to study the surface of NiO-NPs. According to FE-SEM investigation, the particles for NiO-NPs are round and nanoscale in size, Figure 4.

The FE-SEM examination of the NiO-NPs prepared with Lepidium sativum aqueous plant leaves extract is shown the surface characteristics of the NiO-NPs sample. The NiO-NPs are arranged as regular beads in the FE-SEM image, and it is obvious that they are nanometer-sized. The particles are nearly spherical in shape, have uniform sizes, and were found to have an average size of about 42.27 nm, which suggests that the green synthesis method is a successful way to create nickel oxide-nanoparticles. The result was in agreement with Anitha et al. [23] observations of the morphology of the NiO-NPs generated using leaf extract from Thespesia populens. The measurements demonstrated the spherical nature of the NiO-NPs. This study is also agreement with Altaee et al. [24] who used FE-SEM to analyse the shape of NiO-NPs prepared using aloevera leaf extract. The measurements showed that the NiO-NPs were spherical objects with a diameter ranging from 10 to 40 nm.

Figure (4) FE-SEM image showed the shape and size of NiO-NPs.

Atomic force microscopy

Atomic force microscopy (AFM) research revealed that NiO-NPs were spherical, either individually or in aggregates, in both two- and three-dimensional perspectives, and that the average dimeter particle size for NiO-NPs prepared using Lepidium sativum aqueous plant leaves extract was 36.5 nm, Figure 3.

The results were consistent with those of Rahdar et al. [22] who found that the average NiO-nanoparticle size was determined from an AFM picture is 56 nm.

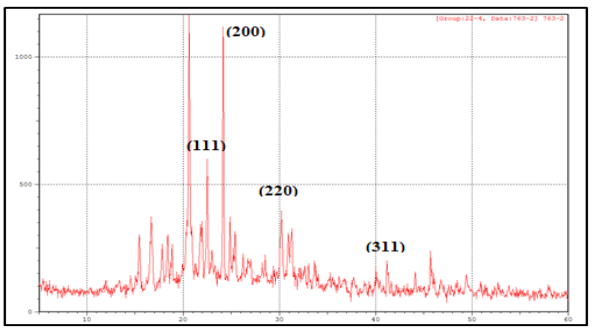

Figure (3): Atomic force microscopy analysis of NiO-NPs (A): Three-dimensional of NiO-NPs, (B): Two-dimensional of NiO-NPs, (C): AFM diagram of size range of NiO-NPs.

X-ray diffractometer (XRD)

The X-ray diffractometer (XRD) is a powerful technology for crystalline material characterization that offers information on structures, phases, preferred crystal orientations, and other structural factors such as average grain size, crystallinity, strain, and crystal defects [25].

The XRD pattern of the NiO-NPs prepared using Lepidium sativum aqueous plant leaves extract is shown in Figure (5). By comparing the XRD peaks with the JCPDS dataset (card No:47-1049), the (111), (200), (220), and (311) planes were identified, clearly indicating NiO-NPs with a cubic structure [26]. The Debye Scherer formula was used to compute the NiO-NPs average crystallite size of the particles from the XRD peak, and the result was 94.47 nm.

The results exhibit nickel oxide XRD patterns. It was discovered that nickel oxide had extremely high and sharp crystalline peaks. Another work's crystalline peak was likewise replicated in the same figure [27]. According to the XRD measurements obtained by Gupta et al. [28], the crystalline size of NiO-NPs is 12.

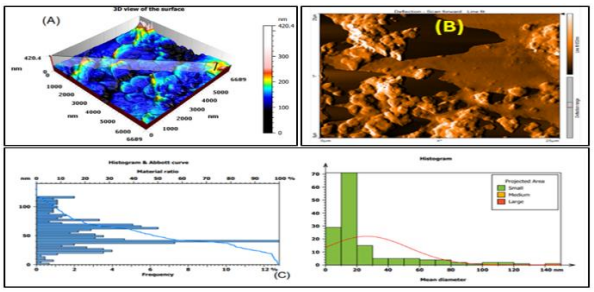

Figure (5): XRD pattern of NiO-NPs

Fourier Transform Infrared (FTIR) Spectroscopy Analysis

The most significant and popular analytical technique for determining the presence of particular functional groups in the produced nanomaterial is FTIR spectroscopy [29].

In certain cases, spectra as low as 400 cm^{-1} (25 µm) were recorded using Fourier Transform Infra-Red (FTIR) spectrophotometers. These spectra were in the range of 4000 cm^{-1} to 670 cm^{-1} (2.5 µm to 15 m). The results of the FTIR Spectra of the Lepidium sativum aqueous plant leaves extract revealed the presence of different functional groups such as Phenolic− OH group stretching, C-H stretching, N-H bend, C-C stretching and C-N stretching. The peaks near 4000 to3200cm−1and 2941 were assigned to O−H stretching and aldehydic C−H stretching, respectively [30], which corresponds to carboxylic acids, primary amines, and alkanes [31]. The peak at 1641 cm^{-1} is (N-H) due to carbonyl stretching in proteins [32], the peak 1384 cm^{-1} corresponding to the C−C stretching bond indicates

the presence of aromatic compounds and the N−O symmetric stretching that demonstrated the presence of the nitro compounds, respectively [33], the peaks 1109 and 1055 were assigned to (OH) and (C-H, C-O)), respectively [34]. The small peaks situated around 1000 cm^{-1} represents the presence of ester. The Smallest peaks 600 cm^{-1} and less indicate the presence of C-Cl stretching of alkyl halides. They had prominent bands of absorbance at peaks (3369.14, 2921.96, 1608.52, 1404.08, and 1029.92) cm^{-1}. In addition, the FTIR Spectra of the $NiSO_4.6H_2O$ had a prominent band of absorbance at peak 1093.56 $cm^{-1.}$ Moreover, the FTIR spectroscopy showed that samples analysis had prominent bands of absorbance at peaks (619.11, 1093.56, 1573.81, 1649.02, and 3365.55) cm^{-1} for the NiO-NPs. The peak (1093.56) in the FTIR Spectra of the NiO-NPs is the same peak found in the $NiSO_4.6H_2O$ sample, and was not found in the Lepidium sativum aqueous plant leaves extract. Therefore, this indicates the formation of NiO-NPs (Figure 6).

A variety of secondary metabolites found in plants, including terpenoids, sugars, polyphenols, alkaloids, proteins, and phenolic acids, are essential for the creation of metal nanoparticles [35].

Results indicate that metal nanoparticles may bind to free carbonyl groups in amino acid residues of proteins found in plant leaf extract while encasing or capping the latter to avoid their aggregation. Certain biological components, including proteins, can reduce metal ions while also stabilizing metal nanoparticles in an aqueous environment. Shankar et al. [36] discovered proteins and secondary metabolites in the water-soluble fractions of Geranium leaves and proved that terpenoids contribute to metal ion reduction and metal ion oxidation to carbonyl groups. According to FTIR study, the chlorophyll ester C=O group acts as a reducing agent, while another protein is involved in the surface capping of metal nanoparticles of Geranium leaf extract. Proteins and other ligands contained in plant extracts were discovered to be responsible for the creation and stability of nanoparticles [37].

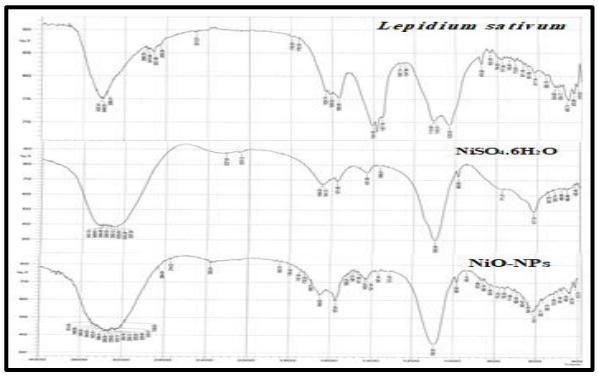

Figure (6): FTIR Spectra Pattern of Lepidium sativum aqueous plant leaves extract, NiSO4.6H2O and NiO-NPs

Antibacterial activity of nickel oxide-nanoparticles

Well diffusion method

The well-diffusion method evaluated the antibacterial activity of the nanoparticles used in this study on S. aureus. The results showed that the NiO-NPs in concentrations 64 mg/ml was more effective than the NiO-NPs in concentrations of 32 mg/ml, which gave the highest inhibition zone value of (15.67 ± 0.57) and (12.33 ± 0.57) mm, respectively, the S. aureus isolate 3, with a significant difference (P≤0.01), as seen in (Tables 3).

Metal nanoparticles' true antibacterial activity's exact mechanism is still unclear. There are, however, a number of papers outlining the potential mechanism behind its antibacterial action. It has been discovered that the antibacterial activity of metal nanoparticles greatly depends on a number of factors, including the particle's size, shape, and surface charge [38]. Particularly in Gram negative bacteria, nanoparticles may readily penetrate the bacterial cell wall and bond with it. Once inside, they inhibit protein synthesize, inactivate the DNA and enzymes, and ultimately cause the bacterial cell to die. Moreover, the huge surface area of nanoparticles allows for robust microbial contact. [39].

Table (3): Antibacterial activity of NiO-NPs on S. aureus isolate

No of isolates	Ni-NPs		LSD value
	32 mg/ml	64 mg/ml	
S_1	11.67±0.57	15.33±0.57	2.170**
S_2	11.33±0.57	14.33±0.57	2.170**
S_3	12.33±0.57	15.67±0.57	2.170**
S_4	9.33±0.57	11.67±0.57	2.170**
S_5	9.33±0.57	11.67±0.57	2.170**
S_6	11.33±0.57	14.67±0.57	2.170**
S_7	11.67±0.57	15.33±0.57	2.170**
S_8	11.33±0.57	14.67±0.57	2.170**
S_9	9.33±0.57	11.67±0.57	2.170**
S_{10}	11.67±0.57	15.33±0.57	2.170**
LSD value	1.341**	1.341**	-------
**(P≤0.01)			

(S): *S. aureus*
The numbers in the table mention to inhibition zone measured in (mm)

By diverting the cell membrane and causing the cell enzymes to be disrupted, nickel oxide-nanoparticles have demonstrated effective prevention of bacterial growth [40]. Abbasi et al. [41], Geranium wallichianum was used as a reducing and capping agent to create ecologically friendly NiO nanoparticles. The NiO nanoparticles used in their investigation were 21 nm in size and shown antibacterial activity against several bacterial strains at doses ranging from 700 to 21.875 g/ml. Bhat et al. [42] synthesized face-centered cubic structure of NiO nanoparticles with 30 nm average size

by co-precipitation method. In their study, K. pneumonia and B. subtilis showed maximum zone of inhibition (15 mm) at 40 mg/ml concentration, and minimum inhibitory concentration 62.5 µg/ml.
This study found that the concentration-dependent antibacterial effects of produced NiO-NPs increased with an increase in concentration and inhibited cellular activity. NiO entered the cell and was poisonous enough to render it inert and dead, which was followed by lysis [43]. Reactive oxygen species (ROS) are produced as a result of the penetration of NiO nanoparticles through bacterial cell membranes, which damages cell components [44]. The size, shape, dose, stability, morphology, and duration of therapy are the primary factors that determine the antibacterial capability of nanoparticles [45].

Determination of the (MIC) of the nickel oxide-nanoparticles

The MIC of the nanoparticles was ascertained utilizing the 96-well microtiter plate and the broth microdilution technique. The MIC of the antibacterial agent S. aureus has been established using a technique utilizing the oxidation-reduction colorimetric indicator resazurin. Resazurin may be easily seen with the naked eye and the MIC can be established even without the use of a spectrophotometer. Resazurin is blue in its oxidized state but becomes pink when reduced by living cells [46].

The result of the MIC values of the NiO-NPs on all S. aureus isolates were 2 mg\ml except isolate 9 which was 4 mg\ml, as shown in (Tables 4) and (Figure 7).

This result shows that the NiO-NPs utilized in this work had efficiency that was concentration dependent, which is consistent with reports of other metal oxide nanoparticles from other studies. [47]. Also, it has been shown that the sizes of nanoparticles significantly influence how effective they are against bacterial [48]. This nanoscale size has a variety of morphologies with large surface area, charge, adsorption, and chemical reactivity that allow them to interact with biological systems effectively and inhibit them significantly [49]. As a result, we infer that the nanoscale diameters of NiO-NPs were critical to their antibacterial efficacy.

Table (4): MIC of NiO-NPs on S. aureus isolate

Isolate	S1	S2	S3	S4	S5	S6	S7	S8	S9	S10
Ni-NPs MIC mg/ml	2	2	2	2	2	2	2	2	4	2

(S): *S. aureus*

No of isolates	Before treatment (control)	After treatment (Ni NPs mg/ml)							
		0.25	0.5	1	2	4	8	16	32
S_1	Strong	Moderate	Weak	Weak	No Biofilm	No Biofilm	No Biofilm	No Biofilm	No Biofilm
S_2	Strong	Moderate	Weak	No Biofilm	No Biofilm	No Biofilm	No Biofilm	No Biofilm	No Biofilm
S_3	Strong	Moderate	Weak	No Biofilm	No Biofilm	No Biofilm	No Biofilm	No Biofilm	No Biofilm
S_4	Strong	Moderate	Weak	No Biofilm	No Biofilm	No Biofilm	No Biofilm	No Biofilm	No Biofilm
S_5	Strong	Moderate	Weak	Weak	No Biofilm	No Biofilm	No Biofilm	No Biofilm	No Biofilm
S_6	Strong	Moderate	Weak	No Biofilm	No Biofilm	No Biofilm	No Biofilm	No Biofilm	No Biofilm
S_7	Strong	Moderate	Weak	Weak	No Biofilm	No Biofilm	No Biofilm	No Biofilm	No Biofilm
S_8	Strong	Moderate	Weak	No Biofilm	No Biofilm	No Biofilm	No Biofilm	No Biofilm	No Biofilm
S_9	Moderate	Moderate	Weak	Weak	No Biofilm	No Biofilm	No Biofilm	No Biofilm	No Biofilm
S_{10}	Moderate	Moderate	Weak	No Biofilm	No Biofilm	No Biofilm	No Biofilm	No Biofilm	No Biofilm

(S): *S. aureus*, Control negative (cut off) = 0.2

Figure (7): MIC of NiO-NPs on S. aureus isolate

(St): Staph. aureus isolate, (C+): Control positive (Bacteria + Media), (C-): Control negative (Media only)

Anti-Biofilm activity of nickel oxide-nanoparticles

A tightly packed group of microbial cells known as a biofilm attaches to and develops on living or nonliving surfaces, and it surrounds itself with secreted polymers. Due to treatment resistance, biofilm-associated infections are sometimes difficult to treat [50], Thus, it is crucial to find novel and potent compounds that prevent the development of bacterial biofilms.

Nickel oxide-nanoparticles inhibited 100% of the biofilm formation of S. aureus in 2 mg/ml, as shown in (Table 5).

The development of biofilms has been linked to bacteria's development of antibiotic resistance [51]. When exposed to NiO-NPs, biofilm formation was lost, which suggests virulence when interacting with and colonizing host tissue. The observed reduction of biofilm development is in line with researches by [52] and [53], they showed that the capacity to suppress biofilm formation and bacterial motility depend on concentration.

Electrostatic interactions are set off when nickel ions produced from NiO-NPs attach to the cell membrane of microorganisms, these interactions affect cellular function [54]. Moreover, these harmed cell membranes are more vulnerable to subsequent interactions, which increases NiO-NPs penetration and intracellular organelle leakage [8]. These consecutive procedures strengthen the nanoparticles' antibacterial properties. Additionally, as NiO-NPs interact, ROS is produced. ROS has a high propensity to interfere with the microbial electron transport chain, damage DNA by rupturing phosphate and hydrogen bonds, denaturize proteins by changing their tertiary structures, and cause oxidative stress to the mitochondria [55]. Although nanoparticles (metal/metal oxide) can readily enter through the bacterial cell membrane and cause the death of the bacterial cell, soluble nickel compounds assault the bacterial cell membrane from the outside [56].

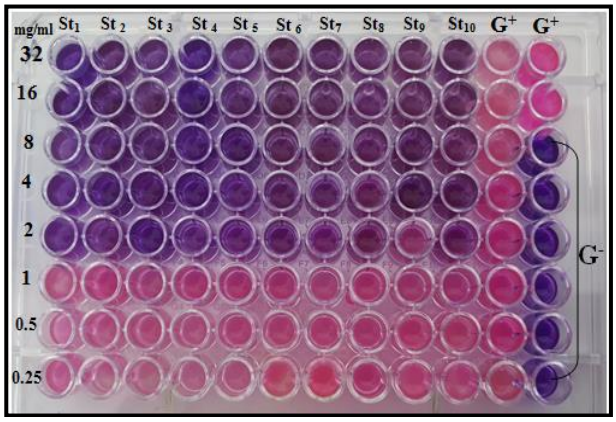

Table (5): Biofilm formation of S. aureus before and after treatment with NiO/NPs

Conclusion

According to the results of the current study, it can be concluded that the green synthesize method is a successful method to prepare NiO-NPs, and the synthesized NiO-NPs have significant antibacterial S. aureus agent, it also inhibits of the formation biofilms in S. aureus depending on the concentration used.

References

Hossain, M. I.; Soliman, M. M.; El-Naggar, M. E.; Sultan, M. Z.; Kechi, A.; Abdelsalam, N. R. and Chowdhury, M. (2021). Synthesis and characterization of graphene oxide-ammonium ferric sulfate composite for the removal of dyes from tannery wastewater. Journal of Materials Research and Technology, May–June; 12:1715-27. DOI:10.1016/J.JMRT.2021.03.097.

Al Saqr, A.; Khafagy, E. S.; Alalaiwe, A.; Aldawsari, M. F.; Alshahrani, S. M.; Anwer, M. K. and Hegazy, W. A. (2021). Synthesis of gold nanoparticles by using green machinery: Characterization and in vitro toxicity. Nanomaterials.; 11(3): 808. https://doi.org/10.3390/nano11030808.

Rónavári, A.; Igaz, N.; Adamecz, D. I.; Szerencsés, B.; Molnar, C.; Kónya, Z. and Kiricsi, M. (2021). Green silver and gold nanoparticles: Biological synthesis approaches and potentials for biomedical applications. Molecules.; 26(4): 844. https://doi.org/10.3390/molecules26040844.

Mosa, W. F.; Ali, H. M. and Abdelsalam, N. R. (2021). The utilization of tryptophan and glycine amino acids as safe alternatives to chemical fertilizers in apple orchards. Environmental Science and Pollution Research., 28(2):1983-91. https://doi.org/10.1007/s11356-020-10658-7.

Tiwari, S. J. and Pawar, S. H. (2014). Nanotechnology applications. Int. J. Pharm. Bio. Sci. 5: 533- 543.

Singh, A., Dubey, S., and Dubey, H. K. (2019). Nanotechnology: The future engineering. Nanotechnology. ; 6(2), 230-3.

Al-Khafaji, A. R. and AL-Azawi, A. H. (2022). Green Method Synthesis of Silver Nanoparticles Using Leaves Extracts of Rosmarinus officinalis. Iraqi Journal of Biotechnology, 21(2): 251-267.

Srihasam, S., Thyagarajan, K., Korivi, M., Lebaka, V. R., and Mallem, S. P. R. (2020). Phytogenic generation of NiO nanoparticles using Stevia leaf extract and evaluation of their in-vitro antioxidant and antimicrobial properties. Biomolecules; 10(1), 89.

Ezhilarasi, A. A., Vijaya, J. J., Kaviyarasu, K., Kennedy, L. J., Ramalingam, R. J. and Al-Lohedan, H. A. (2018). Green synthesis of NiO nanoparticles using Aegle marmelos leaf extract for the evaluation of in-vitro cytotoxicity, antibacterial and photocatalytic properties. Journal of Photochemistry and Photobiology B: Biology ; 180, 39-50.

World Health Organization (WHO). (2003). Basic laboratory procedures in clinical bacteriology. 2nd ed. Genev, Switzerland.

Clinical Laboratory Standards Institute (CLSI). (2019). Performance Standards for Antimicrobial Susceptibility Testing; CLSI Supplement, CLSI M100-28thed., Clinical and Laboratory Standareds Institute Wayne, PA, U.S.A. 39(1).

Patel, F. M., Goswami, P. N. and Khara, R. (2016). Detection of Biofilm formation in device associated clinical bacterial isolates in cancer patients. Sri Lankan Journal of Infectious Diseases, 6(1). 43-50.

Kırmusaoğlu, S. (2019). The methods for detection of biofilm and screening antibiofilm activity of agents. Antimicrobials, antibiotic resistance, antibiofilm strategies and activity methods, 7. 1-17. DOI: http:// dx.doi.org / 10.5772 / intechopen.84411.

Valgas, C.; de Souza, S. M.; Smânia, E. F. A. and Smânia, A. (2007). Screening methods to determine antibacterial activity of natural products. Braz. J. Microbiol., 38: 369–380.

Ohikhena, F. U.; Wintola, O. A. and Afolayan, A. J. (2017). Evaluation of the Antibacterial and Antifungal Properties of Phragmanthera capitata (Sprengel) Balle (Loranthaceae), a Mistletoe Growing on Rubber Tree, Using the Dilution Techniques. The Scientific World Journal, Article ID 9658598. 8 pages doi.org/10.1155/2017/9658598.

Basil AbdulRazzaq, A., Shami, A. M., and Ghaima, K. K. (2022). Detection of vanA and vanB genes Among Vancomycin Resistant Staphylococcus aureus Isolated from Clinical Samples in Baghdad Hospitals. Iraqi journal of biotechnology, 21(1).

Bronowskil, C. James, C. E. and Winstanley, C. (2014). Role of environmental survival in transmission of campylobacter jejuni. FEMS Microbiol. Lett., 356(1). 8-19.

Femi-Adepoju, A. G.; Dada, A. O.; Otun, K. O.; Adepoju, A. O. and Fatoba, O. P. (2019). Green synthesis of silver nanoparticles using terrestrial fern (GleicheniaPectinata (Willd.) C. Presl.): characterization and antimicrobial studies. Heliyon, 5(4): e01543.

Mahmoud, M. A.; Chamanzar, M.; Adibi, A. and El-Sayed, M. A. (2012). Effect of the dielectric constant of the surrounding medium and the substrate on the surface plasmon resonance spectrum and sensitivity factors of highly symmetric systems: silver nanocubes. Journal of the American Chemical Society. 134(14): 6434-6442.

Kumar, V. and Yadav, S. K. (2009). Plant-mediated synthesis of silver and gold nanoparticles and their applications. Journal of Chemical Technology & Biotechnology: International Research in Process, Environmental & Clean Technology, 84(2), 151-157.

Kumar, V. and Yadav, S. K. (2013). Influence of physiochemical factors on size of gold nanoparticles synthesised using leaf extract of Syzygium cumini. Journal of Chemical Science and Technology, 2(1), 104-107.

Rahdar, A., Aliahmad, M. and Azizi, Y. (2015). NiO nanoparticles: synthesis and characterization. Journal of Nanostrucres. 145-151.

Anitha, S. D. C., Lakshmi, V. and Jenila, R. M. (2019). Synthesis of NiO nanoparticles using Thespesia populnea leaves by green synthesis method. International Journal of Research and Development, 4, 70Ā74.

Altaee, M. F., Yaaqoob, L. A., and Kamona, Z. K. (2020). Evaluation of the biological activity of nickel oxide nanoparticles as antibacterial and anticancer agents. Iraqi Journal of Science. 2888-2896.

Salari, S.; Bahabadi, S.E.; Samzadeh-Kermani, A. and Yosefzaei, F. (2019). In-vitro evaluation of antioxidant and antibacterial potential of green synthesized silver nanoparticles using Prosopisfarcta fruit extract. Iranian Journal of Pharmaceutical Research , 18 (1): 430-445.

Qiao, H., Wu, N., Huang, F., Cai, Y. and Wei, Q. (2010). Solvothermal synthesis of NiO/C hybrid microspheres as Li-intercalation electrode material. Materials Letters, 64(9), 1022-1024.

Sun, M., Lan, B., Lin, T., Cheng, G., Ye, F., Yu, L.m et al. (2013). Controlled synthesis of nanostructured manganese oxide: crystalline evolution and catalytic activities. CrystEngComm, 15(35), 7010-7018.

Gupta, V. K., Fakhri, A., Agarwal, S., Ahmadi, E. and Nejad, P. A. (2017). Synthesis and characterization of MnO2/NiO nanocomposites for photocatalysis of tetracycline antibiotic and modification with guanidine for carriers of Caffeic acid phenethyl ester-an anticancer drug. Journal of Photochemistry and Photobiology B: Biology, 174, 235-242.

Fouad H, Li HJ, Hosni D, et al. (2018) Controlling Aedes albopictus and Culex pipiens pallens using silver nanoparticles synthesized from aqueous extract of Cassia fistula fruit pulp and its mode of action. Artif Cells Nanomed Biotechnol. 46:558–567.

Saheed, Y.; Umar, A.F. and Iliyasu, M.Y. (2020). Potential of silver nano particles synthesized from Ficus sycomorus Linn against multidrug resistant Shigella species isolated from clinical specimens. American Journal of Life Sciences, 8(4): 82-90.

Pandey, A.; Sharma, S.K.; Singh, L. and Singh, T.(2013). An overview on Desmostachya bipinnata. J. Drug Discov. Ther. , 7:67–68.

Singh, A.; Mittal, S.; Shrivastava, R.; Dass, S. and Srivastava, J.N. (2012). Biosynthesis of silver nanoparticles using Ricinus communis leaf extract and its antibacterial activity. Digest Journal of Nanomaterials and Biostructures, 7(3): 1157–1163.

Bhumi ,G.; LingaRao, M.and Savithramma N. (2015). Green synthesis of silver nanoparticles from the leaf extract of Adhtoda vasicanees and assessment of its antibacterial activity. Asian J. Pharm. Clin. Res., 8:62–67.

Hadjiivanov, K.I.; Panayotov, D.A.; Mihaylov, M.Y.; Ivanova, E.Z.; Chakarova, K.K.; Andonova, S.M. et al. (2021). Power of infrared and raman spectroscopies to characterize metal organic frameworks and investigate their interaction with guest molecules. Chemical Review,121:1286-1424.

Kuppusamy, P., Yusof, M.M., Maniam, G.P. and Govindan, N. (2014). Biosynthesis of metallic nanoparticles using plant derivatives and their new avenues in pharmacological applications—an updated report. Saudi Pharm. J. 8, 473–484.

Shankar, S.S., Ahmad, A., Pasricha, R. and Sastry, M. (2003). Bioreduction of chloroaurate ions by geranium leaves and its endophytic fungus yields gold nanoparticles of diferent shapes. J. Mater. Chem. 13, 1822–1826.

Mude, N., Ingle, A., Gade, A. and Rai, M. (2009). Synthesis of silver nanoparticles using callus extract of Carica papaya-a frst report. J. Plant Biochem. Biotechnol. 18, 83–86.

Dakal, T. C., Kumar, A., Majumdar, R. S., and Yadav, V. (2016). Mechanistic basis of antimicrobial actions of silver nanoparticles, Front. Microbiol. 7 (2016).

Vega-Jiménez, A. L., Vázquez-Olmos, A. R., Acosta-Gío, E., and Álvarez-Pérez, M. A. (2019). In vitro antimicrobial activity evaluation of metal oxide nanoparticles. Nanoemulsions Prop. Fabr. Appl, 1-18.

Santhoshkumar, A., Kavitha, H. P., & Suresh, R. (2017). Preparation, Characterization and Antibacterial Activity of NiO Nanoparticles. Asian Journal of Chemistry, 29(2).

Abbasi, B. A., Iqbal, J., Mahmood, T., Ahmad, R., Kanwal, S., and Afridi, S. (2019). Plant-mediated synthesis of nickel oxide nanoparticles (NiO) via Geranium wallichianum: Characterization and different biological applications. Materials Research Express, 6(8), 0850a7.

Bhat, S. A., Zafar, F., Mondal, A. H., Kareem, A., Mirza, A. U., Khan, S. et al. (2020). Photocatalytic degradation of carcinogenic Congo red dye in aqueous solution, antioxidant activity and bactericidal effect of NiO nanoparticles. Journal of the Iranian Chemical Society, 17(1), 215-227.

Rakshit, S., Ghosh, S., Chall, S., Mati, S. S., Moulik, S. P. and Bhattacharya, S. C. (2013). Controlled synthesis of spin glass nickel oxide nanoparticles and evaluation of their potential antimicrobial activity: a cost effective and eco-friendly approach. RSC Advances, 3(42), 19348-19356.

Ayeshamariam, A., Sankaracharyulu, G. V., Kashif, M., Hussain, S., Bououdina, M. and Jayachandran, M. (2015). Antibacterial activity studies of Ni and SnO2 loaded Chitosan beads. In Materials Science Forum (Vol. 832, pp. 110-122). Trans Tech Publications Ltd.

Jesudoss, S. K., Vijaya, J. J., Selvam, N., Kombaiah, K., Sivachidambaram, M., Adinaveen, T. and Kennedy, L. J. (2016). Effects of Ba doping on structural, morphological, optical, and photocatalytic properties of self-assembled ZnO nanospheres. Clean Technologies and Environmental Policy, 18(3), 729-741.

Ncube, N. S.; Afolayan, A. J. and Okoh, A. I. (2008). Assessment techniques of antimicrobial properties of natural compounds of plant origin: current methods and future trends. African Journal of Biotechnology, 12(7): 1797-1806.

Ogunyemi, S. O., Zhang, F., Abdallah, Y., Zhang, M., Wang, Y., Sun, G. et al. (2019). Biosynthesis and characterization of magnesium oxide and manganese dioxide nanoparticles using Matricaria chamomilla L. extract and its inhibitory effect on Acidovorax oryzae strain RS-2. Artificial cells, nanomedicine, and biotechnology, 47(1), 2230-2239.

Król, A., Pomastowski, P., Rafińska, K., Railean-Plugaru, V. and Buszewski, B. (2017). Zinc oxide nanoparticles: Synthesis, antiseptic activity and toxicity mechanism. Advances in colloid and interface science, 249, 37-52.

Wang, L., Hu, C. and Shao, L. (2017). The antimicrobial activity of nanoparticles: present situation and prospects for the future. International journal of nanomedicine, 12, 1227.

Kumar, L., Chhibber, S. and K. (2013). Harjai, Zinger one inhibits biofilm formation and improve Antibiofilm efficacy of ciprofloxacin against Pseudomonas aeruginosa PAO1. Fitoterapia, 90. 73–78.

Rajkumari, J., Busi, S., Vasu, A. C. and Reddy, P. (2017). Facile green synthesis of baicalein fabricated gold nanoparticles and their antibiofilm activity against Pseudomonas aeruginosa PAO1. Microbial pathogenesis, 107, 261-269.

Cai, L., Chen, J., Liu, Z., Wang, H., Yang, H. and Ding, W. (2018). Magnesium oxide nanoparticles: effective agricultural antibacterial agent against Ralstonia solanacearum. Frontiers in microbiology, 9, 790.

Al-Khafaji, A. R. and AL-Azawi, A. H. (2022). The Phenolic Compounds Extracted From Rosmarinus officinalis L. and Effect of on The Biofilm Genes in Pseudomonas aeruginosa. Ann. For. Res., 65(1): 1943-1958.

Basak, G., Das, D. and Das, N. (2014). Dual role of acidic diacetate sophorolipid as biostabilizer for ZnO nanoparticle synthesis and biofunctionalizing agent against Salmonella enterica and Candida albicans. Journal of microbiology and biotechnology, 24(1), 87-96.

Burello, E. and Worth, A. P. (2011). A theoretical framework for predicting the oxidative stress potential of oxide nanoparticles. Nanotoxicology, 5(2), 228-235.

Schwerdtle, T. and Hartwig, A. (2006). Bioavailability and genotoxicity of soluble and particulate nickel compounds in cultured human lung cells. Materialwissenschaft und Werkstofftechnik: Entwicklung, Fertigung, Prüfung, Eigenschaften und Anwendungen technischer Werkstoffe, 37(6), 521-525.